Editors' Suggestion

Postselection-Free Entanglement Dynamics via Spacetime Duality

Matteo Ippoliti and Vedika Khemani
Department of Physics, Stanford University, Stanford, California 94305, USA

(Received 30 November 2020; accepted 19 January 2021; published 9 February 2021)

The dynamics of entanglement in "hybrid" nonunitary circuits (for example, involving both unitary gates and quantum measurements) has recently become an object of intense study. A major hurdle toward experimentally realizing this physics is the need to apply *postselection* on random measurement outcomes in order to repeatedly prepare a given output state, resulting in an exponential overhead. We propose a method to sidestep this issue in a wide class of nonunitary circuits by taking advantage of *spacetime duality*. This method maps the purification dynamics of a mixed state under nonunitary evolution onto a particular correlation function in an associated unitary circuit. This translates to an operational protocol which could be straightforwardly implemented on a digital quantum simulator. We discuss the signatures of different entanglement phases, and demonstrate examples via numerical simulations. With minor modifications, the proposed protocol allows measurement of the purity of arbitrary subsystems, which could shed light on the properties of the quantum error correcting code formed by the mixed phase in this class of hybrid dynamics.

DOI: 10.1103/PhysRevLett.126.060501

The dynamics of quantum entanglement is a topical area of research in several subfields of physics ranging from quantum information and quantum gravity to condensed matter and atomic physics [1–13]. Recent works have begun to extend this line of research to *nonunitary* settings, involving many-body systems subject to repeated measurements [14–40]. Remarkably, this has led to the discovery of novel entanglement phase transitions in the dynamics of open quantum systems modeled by circuits of random unitary gates interleaved with local projective measurements [14–16]. These monitored dynamics exhibit a phase transition as a function of the measurement rate, separating a "disentangling" phase (where the entanglement entropy obeys an area-law) from an "entangling" phase (where it obeys a volume law). These phases and transitions are only visible in individual quantum trajectories [41], corresponding to particular sequences of measurement outcomes. Such "monitored dynamics" are an essential feature of near-term quantum devices in which modulated interactions with an environment, say via measurements, are necessary for unitary control and feedback. Many questions, both on the transition and on the steady-state phases themselves, remain active areas of study—notably the universality class of the transitions [21,22,31] and the nature of the volume-law phase, which is understood as a dynamically generated quantum error-correcting code (QECC) hiding information from local measurements [17–19,26,38].

Measuring entanglement generally requires the preparation of many identical copies of the same state (either simultaneously or sequentially) [42–53]. In the presence of measurements, this becomes extremely challenging as it requires *postselection*: a quantum measurement is an intrinsically random process whose outcomes are sampled stochastically with Born probabilities, and a quantum trajectory in this evolution is associated with a *specific* record of measurement outcomes. Hence, preparing multiple copies of the same state incurs an exponential postselection overhead $e^{O(pLT)}$ in the size L and depth T of the circuit (assuming a finite rate of measurement p). There are ways to partly overcome this challenge: (i) using a single reference qubit as a *local probe* of the entanglement phase transition [20], which considerably alleviates the postselection overhead; (ii) in Clifford circuits, using a combination of classical simulations and feedback to force specific measurement outcomes by error correcting any "wrong" ones. Nevertheless, it is still desirable to *directly* access the entanglement properties of more general nonunitary and non-Clifford evolutions.

In this Letter, we propose a novel method to access quantum entanglement in a broad class of nonunitary circuits *without* facing an exponential postselection barrier. Specifically, we will consider nonunitary circuits that are *"spacetime dual"* (explained below) to unitary evolutions; and we propose a method for measuring the purity $\mathrm{Tr}(\rho^2)$, related to the second Renyi entropy via $\mathrm{Tr}(\rho^2) = e^{-S_2(\rho)}$, for the whole system as well as for arbitrary subsystems. This allows access to the purification dynamics of an initially mixed state, which is intimately related to the entanglement dynamics of pure states [18]. In particular, the volume-law entangled phase maps onto the *mixed* phase, in which the dynamics generates a QECC that protects information from measurements, so that an initially mixed state remains mixed for exponentially long times. Subsystem purity measurements contain key information about the nature of this as-of-yet poorly understood QECC [18,26,38].

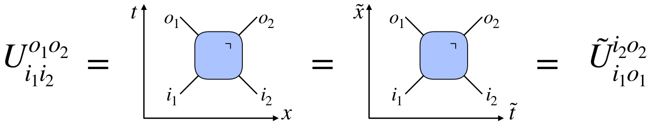

FIG. 1. Spacetime duality. By swapping the spatial and temporal axes, a unitary gate U maps onto another, generally nonunitary gate $\tilde{U}$.

We note that while the class of nonunitary circuits for which our method applies is not completely general, it still encompasses a broad space. To every unitary circuit comprised of nearest-neighbor two-qubit gates, we can associate a spacetime-dual circuit (see below) which is generically nonunitary [54]. Because this is a one-to-one correspondence, the space of hybrid models we consider is as large as the space of unitary circuits built from local two-qubit gates. In particular our results apply to circuits with (a specific class of) unitary gates interspersed with (specific types of) forced projective measurements.

Spacetime duality.—Given a two-qubit unitary gate $U_{i_1,i_2}^{o_1,o_2}$, mapping input qubits $i_{1,2}$ (bottom legs) to output qubits $o_{1,2}$ (top legs), we define its spacetime dual $\tilde{U}$ as the matrix obtained by flipping the arrow of time by 90°, i.e., viewing the left legs as inputs and the right legs as outputs: $U_{i_1,i_2}^{o_1,o_2} \equiv \tilde{U}_{i_1,o_1}^{i_2,o_2}$ (Fig. 1). The result of this transformation, $\tilde{U}$, is generally not unitary (gates U such that $\tilde{U}$ is also unitary are known as "dual unitary" and have been studied intensely recently [55–62]). The generic nonunitarity of $\tilde{U}$, and the possibility that it might counter entanglement growth, has also been employed to pursue more efficient tensor network contraction schemes [63,64], and similar ideas were applied to study the complexity of shallow $(2+1)$-dimensional circuits [65].

In general, one has $\tilde{U} \equiv 2VH$, where V is unitary and H is a positive semidefinite matrix of unit norm, which can be seen as a generalized measurement (i.e., an element of a POVM set [66]; see Ref. [67] for more details). As an example, $U = \mathbb{1}$ yields $\tilde{U} = 2|B^+\rangle\langle B^+|$, where $|B^+\rangle = (|00\rangle + |11\rangle)/\sqrt{2}$ is a Bell pair state. Thus the spacetime duality transformation generally maps unitary circuits to nonunitary *hybrid circuits* involving unitary gates as well as (weak or projective) measurements, up to prefactors. Crucially, the measurements are *forced*: the outcome is deterministic; no quantum randomness is involved. In the example of $U = \mathbb{1}$, the outcome is always $|B^+\rangle$. The ability to avoid postselection in our protocol stems from this observation.

Postselection-free measurement protocol.—The idea is to use a "laboratory" system, whose evolution is unitary, to simulate a "dual" system whose evolution is nonunitary and realizes purification dynamics. We will use t ($\tilde{t}$) do denote the arrow of time in the unitary (nonunitary) evolution. The target purification dynamics starts with a fully mixed state, $\rho_{\rm in} = \mathbb{1}/2^{\tilde{L}}$ on an even number $\tilde{L}$ of qubits (we use a tilde for quantities defined in the nonunitary time direction) [68]. This is evolved by a nonunitary circuit including forced measurements, M. The output state, $\rho_{\rm out} \propto MM^\dagger$ [Fig. 2(a)], may be partially or completely purified. We focus on nonunitary circuits M whose spacetime dual is a unitary circuit, i.e., $M = \tilde{U}_M$ with U_M unitary; in this case, it is possible to view $\rho_{\rm out}$ as living on a timelike slice at the spatial edge of a unitary circuit [Fig. 2(b)]. Likewise the purity, ${\rm Tr}({\rho_{\rm out}}^2)$ [Fig. 2(c)], maps under spacetime duality to a (multipoint) correlation function in an associated unitary evolution [Fig. 2(d)]: a bipartite one-dimensional chain in which the left half evolves under the unitary U_M, the right half evolves under RU_M^*R (R denotes spatial inversion), and the only region where the evolution is nonunitary is the central pair of qubits, where horizontal bonds (spacelike qubit worldlines) implement the product of $\rho_{\rm out}$ with itself. We additionally note that unitarity of U_M (coupled with special *"depolarizing"* boundary conditions, discussed in detail in the Supplemental Material [54]) elides all gates outside forward and backward lightcones emanating from the central pair of qubits, as in Fig. 2(e).

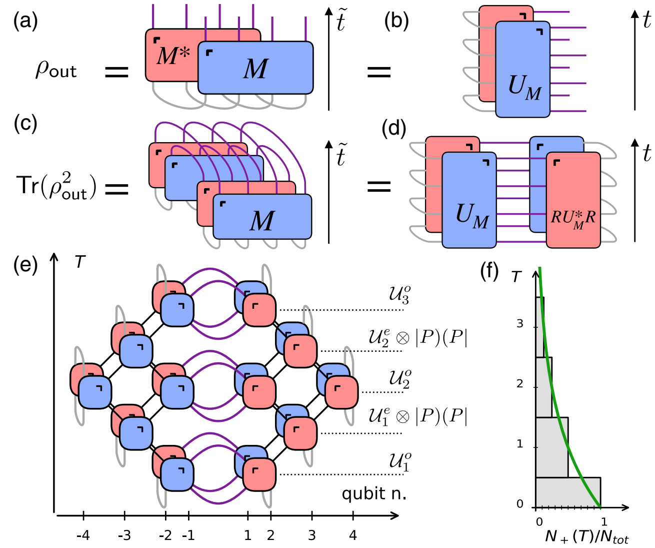

FIG. 2. (a) Purification dynamics: a fully mixed state $\rho_{\rm in} \propto \mathbb{1}$ (gray lines, bottom) is evolved by a hybrid circuit M, yielding a state $\rho_{\rm out} \propto MM^\dagger$ (purple lines, top). (b) If $M = \tilde{U}_M$ with U_M unitary, the purification process is spacetime dual to a unitary evolution. $\rho_{\rm out}$ lives on a timelike slice of the circuit (purple legs, right). (c) Purity of the output state, ${\rm Tr}(\rho_{\rm out}^2)$. (d) Same tensor network viewed as a correlation function in a unitary circuit. The arrow of time $\tilde{t}$ (t) denotes hybrid (unitary) evolution. (e) Protocol for measuring the purity of $\rho_{\rm out}$, sketched for $T = 3$. Tensor network legs are color coded as in (a)–(d). Qubits ± 1 are repeatedly initialized in the Bell state $P = |B^+\rangle\langle B^+|$ (upward purple arcs) and measured in the Bell basis (downward purple arcs); the protocol succeeds if all T Bell measurements yield $|B^+\rangle$. (f) The fraction of runs that are successful up to time T, $N_+(T)/N_{\rm tot}$, yields the purity of $\rho_{\rm out}$ on $\tilde{L} = 2T$ qubits.

The goal of the following discussion is to provide an interpretation of the nonunitary processes taking place at the central bond, so that this tensor contraction can be converted into an operational prescription for the measurement of the purity. In the laboratory (unitary) time direction, one has a chain of $L \equiv \tilde{L} + 2$ qubits evolved for time $T \equiv \tilde{L}/2$. We symmetrically label the qubits as $i = \{\pm 1, \pm 2, \ldots \pm (T+1)\}$, and denote qubits $i \leq -2$ as $\mathcal{L}$ (left), $i = \pm 1$ as $\mathcal{C}$ (central), and $i \geq 2$ as $\mathcal{R}$ (right). The system is initialized in the state $\rho \propto \mathbb{1}_{\mathcal{L}} \otimes P_{\mathcal{C}} \otimes \mathbb{1}_{\mathcal{R}}$, where $P = |B^+\rangle\langle B^+|$ and $|B^+\rangle = (1/\sqrt{2})(|00\rangle + |11\rangle)$ is a Bell state. It is then evolved in time by a circuit with a brickwork structure. First a layer of unitary gates, represented by superoperator $\mathcal{U}_t^o$, acts on the "odd" bonds—a layer of the circuit U_M on $\mathcal{L} \cup \{-1\}$ and a layer of $RU_M^* R$ on $\mathcal{R} \cup \{+1\}$. Next, a similarly defined unitary layer $\mathcal{U}_t^e$ acts on "even" bonds, which do not include $\mathcal{C}$. There, a *forced* Bell measurement takes place: $\rho \mapsto P_{\mathcal{C}} \otimes \mathrm{Tr}_{\mathcal{C}}(P_{\mathcal{C}}\rho)$. The process terminates at time $t = T$ with a final forced measurement of $P_{\mathcal{C}}$. Using the operator-state representation, in which $|A)$ denotes an operator A as a state with inner product $(A|B) = \mathrm{Tr} A^\dagger B$, the forced Bell measurement reads $|\rho) \mapsto |P_{\mathcal{C}})(P_{\mathcal{C}}|\rho)$, and the overall evolution can be written as

$$\mathrm{Tr}(\rho_{\mathrm{out}}^2) \propto (P|\mathcal{U}_T^o \circ \prod_{t=1}^{T-1} [\mathcal{U}_t^e \otimes |P_{\mathcal{C}})(P_{\mathcal{C}}|] \circ \mathcal{U}_t^o|P), \quad (1)$$

where $|P) \equiv |P_{\mathcal{C}}) \otimes |\mathbb{1}_{\mathcal{L}\cup\mathcal{R}})$. The purity of the hybrid circuit output ρ_{out} is thus mapped to a $(2T)$-point correlation function of the projector $P_{\mathcal{C}}$ during a unitary evolution obtained from the original hybrid circuit M via the spacetime duality.

We are now in a position to recast the result in Eq. (1) as an operational protocol for measuring the purity of the state of interest, ρ_{out}. The protocol consists of the following steps: (i) Choose an integer T and prepare a $2(T+1)$-qubit chain in the state $\rho = \mathbb{1}_{\mathcal{L}} \otimes P_{\mathcal{C}} \otimes \mathbb{1}_{\mathcal{R}}/4^T$. Set $t = 1$. (ii) Evolve odd bonds unitarily under $\mathcal{U}_t^o$. (iii) Perform a Bell measurement on $\mathcal{C}$. If the outcome is $|B^+\rangle$, continue; otherwise, stop and record a failure. (iv) If $t = T$, stop and record a success; otherwise, evolve even bonds unitarily under $\mathcal{U}_t^e$, increment t by one, and go back to step (ii). Let the number of "successful" runs out of N_{tot} trials be $N_+(T)$; then,

$$\mathrm{Tr}(\rho_{\mathrm{out}}^2|_{\tilde{L}=2T,\tilde{T}=T}) = N_+(T)/N_{\mathrm{tot}}, \quad (2)$$

where $\rho_{\mathrm{out}}|_{\tilde{L}=2T,\tilde{T}=T}$ denotes the output state of hybrid dynamics on a system of $\tilde{L} = 2T$ qubits evolved for time $\tilde{T} = T$. This is the central result of this Letter. Note that while we have not kept track of numerical prefactors in this derivation, the proportionality constant in Eq. (2) turns out to be exactly one, see Ref. [54].

We emphasize that the above protocol, despite featuring projective measurements and runs ending in "failure," does *not* use postselection. Indeed, failures increment the denominator N_{tot} in Eq. (2) and provide crucial information for the purity measurement. In other words, copies of the same state ρ_{out} (identical up to control errors) can be realized deterministically arbitrarily many times. The exponential overhead of postselection is entirely removed. Finally, we remark that if one wants to prepare ρ_{out} in real space (as opposed to a timelike slice of the circuit as obtained above), this can be achieved with an approach based on gate teleportation [66], using $2T$ ancillas initialized in $|B^+\rangle$ Bell states and $O(T^2)$ SWAP gates in a 1D geometry; see Ref. [54].

Entanglement phases.—While a typical hybrid circuit is generally *not* dual to a unitary circuit, the space of models we address is still very large, and it is reasonable to expect a rich variety of purification phases and entanglement phenomena within this class of models. Here we begin to explore this space for the purpose of demonstrating that interesting purification phases are indeed possible, while leaving the longer-term enterprise of charting this space to future work.

Surprisingly, despite the presence of measurements, Eq. (2) suggests that the generic outcome of the purification dynamics in these models should be a mixed phase, in which ρ_{out} has extensive entropy. Indeed, if the late-time probability of obtaining $|B^+\rangle$ as the outcome of the Bell measurement on $\mathcal{C}$ approaches any value $p_\infty < 1$, then $N_+(T)$—which requires the outcome of *all* T Bell measurements to be $|B^+\rangle$—decays exponentially at late times. Therefore the state has a finite entropy density s_2 directly measurable from a decay time constant:

$$\mathrm{Tr}(\rho_{\mathrm{out}}^2|_{\tilde{L}=2T,\tilde{T}=T}) \sim e^{-T/\tau} \Rightarrow s_2 \equiv (2\tau)^{-1}. \quad (3)$$

This is another main result of this Letter.

The mixed-phase outcome should be expected whenever the unitary circuit U_M features any amount of scrambling: then, any projector $|B^+\rangle\langle B^+|$ injected in $\mathcal{C}$ will irreversibly grow into a global operator, never refocusing at $\mathcal{C}$; thus the probability of later obtaining $|B^+\rangle$ as a Bell measurement outcome will be lower than 1, and the above argument will give a mixed phase. However, exceptions are possible in nonscrambling circuits.

As an illustration, we map out the purification phases for a specific model. For computational simplicity and closer comparison with the known phenomenology, we choose a set of unitary Clifford circuits whose spacetime duals consist only of unitary gates and projective Pauli measurements. We consider a brickwork layer of two-qubit Clifford gates chosen as indicated in Fig. 3(a): $\mathrm{Prob}(\mathbb{1}) = p$, $\mathrm{Prob}(\mathrm{iSWAP}) = (1-p)J/2$ [69], $\mathrm{Prob}(\mathrm{SWAP}) = (1-p)(1-J/2)$. Random single-qubit Clifford gates act before and after each two-qubit gate so there are no symmetries in the model. As SWAP and iSWAP are dual unitary while $\tilde{\mathbb{1}} \propto |B^+\rangle\langle B^+|$ is a projector, $p \in [0,1]$ serves as the measurement rate for the dual

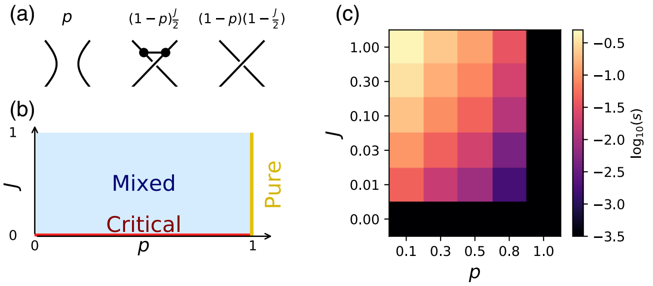

FIG. 3. (a) Summary of the Clifford circuit model: probabilities of $\mathbb{1}$, iSWAP and SWAP gates. (b) Schematic of purification phase diagram of the dualized circuit vs p, J. (c) Entropy density of hybrid circuit output state ρ_{out} vs p, J (Clifford simulations on $\tilde{L} \leq 4096$ qubits).

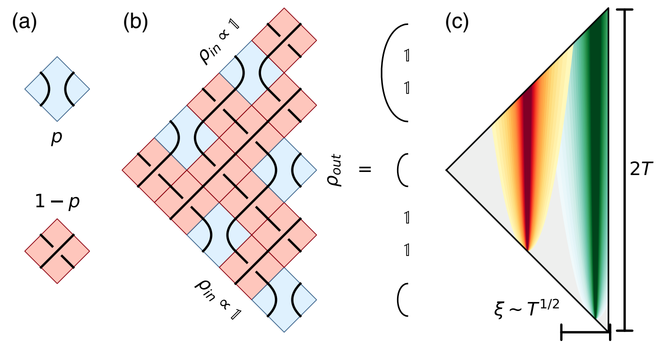

FIG. 4. Critical phase of the noninteracting ($J = 0$) Clifford circuit model. (a) Allowed gates, $\mathbb{1}$ (blue tile) and SWAP (red tile). (b) A realization of the circuit for $T = 5$. The purification dynamics proceeds left to right; the input qubit worldlines (ρ_{in}, left) are fully mixed; the output state (ρ_{out}, right) contains Bell pairs (arcs) and fully mixed qubits ($\mathbb{1}$ symbols). (c) Coarse-grained view of the purification dynamics ($T \gg 1$). Only qubit worldlines that enter within a distance $\xi \sim T^{1/2}$ of ρ_{out} (e.g., green shaded parabola) are likely to diffuse to ρ_{out} and contribute entropy.

hybrid circuit. $J \in [0, 1]$ serves as an interaction rate, with $J = 0$ giving a noninteracting "swap circuit." We note that the spacetime dual of this unitary model is not too different from the original unitary-projective model considered in Ref. [14]: single-site Z measurements are replaced by two-qubit Bell measurements; gates are sampled out of exactly half of the two-qubit Clifford group, rather than the whole group. Remarkably, these seemingly small changes yield a completely different phase diagram, sketched in Fig. 3(b).

Via stabilizer numerical simulations we find three possible outcomes across the (p, J) parameter space [results for the entropy density are shown in Fig. 3(c)]. A pure phase is only possible at $p = 1$, where the circuit U_M consists purely of identity gates and $\rho_{\text{out}} = (|B^+\rangle\langle B^+|)^{\otimes T}$ is trivially a pure state. Remarkably, it is unstable to infinitesimal perturbations away from $p = 1$, in sharp contrast to other unitary-projective models where the pure phase is generic for sufficiently high measurement rates. For any $J > 0$ and $p < 1$ (i.e., almost all of parameter space) we have a mixed phase: indeed, this is the default outcome for generic interacting circuits. Finally, on the $J = 0$ (and $0 < p < 1$) line, we have a critical purification phase, with vanishing entropy density $s_2 = 0$ but divergent entropy $S_2 \sim \sqrt{T}$, which we characterize in the following.

Setting $J = 0$, the circuit maps to a loop model with two tiles, one associated to $\mathbb{1}$ (probability p) and one to SWAP (probability $1 - p$), see Fig. 4(a); the qubits move ballistically under SWAP gates and backscatter under $\mathbb{1}$, thus tracing random walks with step size ℓ distributed exponentially, $\text{Prob}(\ell) \propto (1 - p)^{|\ell|}$. Worldlines that begin and end in ρ_{out} define a pure Bell pair entirely contained in the system, and thus contribute no entropy; on the contrary, wordlines that begin at the lightcone boundaries (ρ_{in}) and terminate in ρ_{out}, or vice versa, yield a fully mixed qubit in the output state and thus contribute one bit of entropy [Fig. 4(b)]. How many such worldlines are there? Because the qubits undergo diffusion [70], only those that enter the dynamics within $O(T^{1/2})$ steps of ρ_{out} are likely to contribute entropy, see Fig. 4(c). Thus we have $S_2(T) \sim \sqrt{T}$, and a stretched-exponential purification dynamics $\text{Tr}({\rho_{\text{out}}}^2) \sim e^{-c\sqrt{T}}$, to be compared with the exponential decay in the mixed phase.

Subsystem purity and quantum code properties.— Having established the existence (and prevalence) of the mixed phase in this class of models, it is interesting to investigate its properties, especially since the nature of the QECC defining the mixed phase remains in general poorly understood [19,26,38]. To access such properties in experiment, one needs to measure not only the entropy of the entire state, but also of different subsystems.

First we note that for *contiguous*, *even-sized* subsystems of the temporal slice where ρ_{out} lives, $A = \{0 \leq \tau < 2t_A\}$, the subsystem purity obeys $\text{Tr}(\rho_{\text{out},A}^2) = N(t_A)/N_{\text{tot}}$, and is therefore obtained for all $t_A \leq T$, at no additional cost, by running the protocol up to time T. This follows from elision of all gates that lie outside a light cone ending in A, see Ref. [54].

To access general bipartitions, the protocol must be slightly modified. The key idea is to "trace out" qubits in the complement of the subsystem of interest $\bar{A}$ by means of depolarization, e.g., by averaging over random unitary gates (see Ref. [54]). We find that

$$\text{Tr}(\rho_{\text{out},A}^2) = 2^{n_e - n_o} N_+(T; A)/N_{\text{tot}}, \tag{4}$$

where n_e (n_o) is the number of even (odd) qubits in partition $\bar{A}$, on which a Bell pair is initialized (measured), and $N_+(T; A)$ is the number of successful runs based on a modified criterion: the protocol *cannot* fail on any of the n_o Bell measurements in the partition $\bar{A}$; if a state other than $|B^+\rangle$ is obtained in such steps, it is reset to $|B^+\rangle$ and the protocol continues instead of failing [54].

The purity for such noncontiguous bipartitions in stabilizer states can be used to obtain the contiguous code distance d_{cont}, an important property of the QECC that protects the mixed phase (see Ref. [54]). Numerically, we find that ρ_{out} in the mixed phase defines a code with a power-law divergent, subextensive mutual information and contiguous distance (in the bulk of the system), similar to the phenomenology of the mixed phase in other Clifford models [26,38].

Discussion.—We have shown that a large class of nonunitary circuits allows direct experimental access to purification dynamics without postselection, thus sidestepping a major obstacle toward the observation of entanglement phases in monitored circuits. This is achieved by viewing the (nonunitary) spacetime duals of unitary gates as forced measurements. Our protocol can be used to measure the purity of the whole system as well as arbitrary subsystems, and could enable the experimental investigation of the spatial entanglement structure and QECC properties in the mixed phase of these models.

While the class of models we study is a measure-zero subset of all nonunitary circuits, it is nonetheless very large —in one-to-one correspondence with the space of local unitary circuits. In this Letter we have studied a simple family of models as a demonstration; a thorough exploration of this vast space and of the types of entanglement dynamics it may contain is a fascinating direction for future work.

We thank Sarang Gopalakrishnan, Michael Gullans, David Huse, Xiaoliang Qi, Tibor Rakovszky, and Dominic Williamson for valuable discussions. This work was supported with funding from the Defense Advanced Research Projects Agency (DARPA) via the DRINQS program (M. I.) and the U.S. Department of Energy, Office of Science, Basic Energy Sciences, under Early Career Award No. DE-SC0021111 (V. K.). The views, opinions and/or findings expressed are those of the authors and should not be interpreted as representing the official views or policies of the Department of Defense or the U.S. Government. M. I. was funded in part by the Gordon and Betty Moore Foundations EPiQS Initiative through Grants No. GBMF4302 and GBMF8686. Numerical simulations were performed on Stanford Research Computing Center's Sherlock cluster.

[1] R. Horodecki, P. Horodecki, M. Horodecki, and K. Horodecki, Quantum entanglement, Rev. Mod. Phys. **81**, 865 (2009).

[2] L. Amico, R. Fazio, A. Osterloh, and V. Vedral, Entanglement in many-body systems, Rev. Mod. Phys. **80**, 517 (2008).

[3] J. Eisert, M. Cramer, and M. B. Plenio, Colloquium: Area laws for the entanglement entropy, Rev. Mod. Phys. **82**, 277 (2010).

[4] P. Calabrese and J. Cardy, Entanglement entropy and conformal field theory, J. Phys. A **42**, 504005 (2009).

[5] J. H. Bardarson, F. Pollmann, and J. E. Moore, Unbounded Growth of Entanglement in Models of Many-Body Localization, Phys. Rev. Lett. **109**, 017202 (2012).

[6] H. Kim and D. A. Huse, Ballistic Spreading of Entanglement in a Diffusive Nonintegrable System, Phys. Rev. Lett. **111**, 127205 (2013).

[7] T. Hartman and J. Maldacena, Time evolution of entanglement entropy from black hole interiors, J. High Energy Phys. 2013 (2013) 14.

[8] H. Liu and S. J. Suh, Entanglement Tsunami: Universal Scaling in Holographic Thermalization, Phys. Rev. Lett. **112**, 011601 (2014).

[9] M. Mezei and D. Stanford, On entanglement spreading in chaotic systems, J. High Energy Phys. 2017 (2017) 65.

[10] A. Nahum, J. Ruhman, S. Vijay, and J. Haah, Quantum Entanglement Growth Under Random Unitary Dynamics, Phys. Rev. X **7**, 031016 (2017).

[11] C. W. von Keyserlingk, T. Rakovszky, F. Pollmann, and S. L. Sondhi, Operator Hydrodynamics, Otocs, and Entanglement Growth in Systems Without Conservation Laws, Phys. Rev. X **8**, 021013 (2018).

[12] Y. Huang, Dynamics of renyi entanglement entropy in local quantum circuits with charge conservation, IOP SciNotes **1**, 035205 (2020).

[13] A. R. Brown, H. Gharibyan, S. Leichenauer, H. W. Lin, S. Nezami, G. Salton, L. Susskind, B. Swingle, and M. Walter, Quantum gravity in the lab: Teleportation by size and traversable wormholes, arXiv:1911.06314.

[14] Y. Li, X. Chen, and M. P. A. Fisher, Quantum zeno effect and the many-body entanglement transition, Phys. Rev. B **98**, 205136 (2018).

[15] B. Skinner, J. Ruhman, and A. Nahum, Measurement-Induced Phase Transitions in the Dynamics of Entanglement, Phys. Rev. X **9**, 031009 (2019).

[16] Y. Li, X. Chen, and M. P. A. Fisher, Measurement-driven entanglement transition in hybrid quantum circuits, Phys. Rev. B **100**, 134306 (2019).

[17] S. Choi, Y. Bao, X.-L. Qi, and E. Altman, Quantum Error Correction in Scrambling Dynamics and Measurement-Induced Phase Transition, Phys. Rev. Lett. **125**, 030505 (2020).

[18] M. J. Gullans and D. A. Huse, Dynamical Purification Phase Transition Induced by Quantum Measurements, Phys. Rev. X **10**, 041020 (2020).

[19] R. Fan, S. Vijay, A. Vishwanath, and Y.-Z. You, Self-organized error correction in random unitary circuits with measurement, arXiv:2002.12385.

[20] M. J. Gullans and D. A. Huse, Scalable Probes of Measurement-Induced Criticality, Phys. Rev. Lett. **125**, 070606 (2020).

[21] Y. Bao, S. Choi, and E. Altman, Theory of the phase transition in random unitary circuits with measurements, Phys. Rev. B **101**, 104301 (2020).

[22] C.-M. Jian, Y.-Z. You, R. Vasseur, and A. W. W. Ludwig, Measurement-induced criticality in random quantum circuits, Phys. Rev. B **101**, 104302 (2020).

[23] X. Cao, A. Tilloy, and A. De Luca, Entanglement in a fermion chain under continuous monitoring, SciPost Phys. **7**, 24 (2019).

[24] A. Nahum and B. Skinner, Entanglement and dynamics of diffusion-annihilation processes with majorana defects, Phys. Rev. Research **2**, 023288 (2020).

[25] A. Zabalo, M. J. Gullans, J. H. Wilson, S. Gopalakrishnan, D. A. Huse, and J. H. Pixley, Critical properties of the measurement-induced transition in random quantum circuits, Phys. Rev. B **101**, 060301(R) (2020).

[26] M. Ippoliti, M. J. Gullans, S. Gopalakrishnan, D. A. Huse, and V. Khemani, Entanglement Phase Transitions in Measurement-Only Dynamics, Phys. Rev. X (to be published).

[27] A. Lavasani, Y. Alavirad, and M. Barkeshli, Measurement-induced topological entanglement transitions in symmetric random quantum circuits, Nat. Phys. https://doi.org/10.1038/s41567-020-01112-z (2021).

[28] S. Sang and T. H. Hsieh, Measurement protected quantum phases, arXiv:2004.09509.

[29] Q. Tang and W. Zhu, Measurement-induced phase transition: A case study in the nonintegrable model by density-matrix renormalization group calculations, Phys. Rev. Research **2**, 013022 (2020).

[30] J. Lopez-Piqueres, B. Ware, and R. Vasseur, Mean-field entanglement transitions in random tree tensor networks, Phys. Rev. B **102**, 064202 (2020).

[31] Y. Li, X. Chen, A. W. W. Ludwig, and M. P. A. Fisher, Conformal invariance and quantum non-locality in hybrid quantum circuits, arXiv:2003.12721.

[32] X. Turkeshi, R. Fazio, and M. Dalmonte, Measurement-induced criticality in $(2+1)$-dimensional hybrid quantum circuits, Phys. Rev. B **102**, 014315 (2020).

[33] O. Alberton, M. Buchhold, and S. Diehl, Trajectory dependent entanglement transition in a free fermion chain—from extended criticality to area law, arXiv:2005.09722.

[34] Y. Fuji and Y. Ashida, Measurement-induced quantum criticality under continuous monitoring, Phys. Rev. B **102**, 054302 (2020).

[35] O. Lunt and A. Pal, Measurement-induced entanglement transitions in many-body localized systems, Phys. Rev. Research **2**, 043072 (2020).

[36] M. Szyniszewski, A. Romito, and H. Schomerus, Universality of Entanglement Transitions from Stroboscopic to Continuous Measurements, Phys. Rev. Lett. **125**, 210602 (2020).

[37] S. Vijay, Measurement-driven phase transition within a volume-law entangled phase, arXiv:2005.03052.

[38] Y. Li and M. P. A. Fisher, Statistical mechanics of quantum error-correcting codes, arXiv:2007.03822.

[39] L. Fidkowski, J. Haah, and M. B. Hastings, How dynamical quantum memories forget, Quantum **5**, 382 (2021).

[40] A. Nahum, S. Roy, B. Skinner, and J. Ruhman, Measurement and entanglement phase transitions in all-to-all quantum circuits, on quantum trees, and in Landau-Ginsburg theory, arXiv:2009.11311.

[41] J. Dalibard, Y. Castin, and K. Mølmer, Wave-Function Approach to Dissipative Processes in Quantum Optics, Phys. Rev. Lett. **68**, 580 (1992).

[42] P. Horodecki, Measuring Quantum Entanglement Without Prior State Reconstruction, Phys. Rev. Lett. **90**, 167901 (2003).

[43] A. J. Daley, H. Pichler, J. Schachenmayer, and P. Zoller, Measuring Entanglement Growth in Quench Dynamics of Bosons in an Optical Lattice, Phys. Rev. Lett. **109**, 020505 (2012).

[44] D. A. Abanin and E. Demler, Measuring Entanglement Entropy of a Generic Many-Body System with a Quantum Switch, Phys. Rev. Lett. **109**, 020504 (2012).

[45] S. J. van Enk and C. W. J. Beenakker, Measuring $\mathrm{Tr}\rho^n$ on Single Copies of ρ using Random Measurements, Phys. Rev. Lett. **108**, 110503 (2012).

[46] R. Islam, R. Ma, Philipp M. Preiss, M. Eric Tai, A. Lukin, M. Rispoli, and M. Greiner, Measuring entanglement entropy in a quantum many-body system, Nature (London) **528**, 77 (2015).

[47] A. M. Kaufman, M. E. Tai, A. Lukin, M. Rispoli, R. Schittko, P. M. Preiss, and M. Greiner, Quantum thermalization through entanglement in an isolated many-body system, Science **353**, 794 (2016).

[48] N. M. Linke, S. Johri, C. Figgatt, K. A. Landsman, A. Y. Matsuura, and C. Monroe, Measuring the rényi entropy of a two-site fermi-hubbard model on a trapped ion quantum computer, Phys. Rev. A **98**, 052334 (2018).

[49] A. Elben, B. Vermersch, M. Dalmonte, J. I. Cirac, and P. Zoller, Rényi Entropies from Random Quenches in Atomic Hubbard and Spin Models, Phys. Rev. Lett. **120**, 050406 (2018).

[50] T. Brydges, A. Elben, P. Jurcevic, B. Vermersch, C. Maier, B. P. Lanyon, P. Zoller, R. Blatt, and C. F. Roos, Probing rényi entanglement entropy via randomized measurements, Science **364**, 260 (2019).

[51] A. Elben, B. Vermersch, C. F. Roos, and P. Zoller, Statistical correlations between locally randomized measurements: A toolbox for probing entanglement in many-body quantum states, Phys. Rev. A **99**, 052323 (2019).

[52] A. Elben, R. Kueng, H.-Y. R. Huang, R. van Bijnen, C. Kokail, M. Dalmonte, P. Calabrese, B. Kraus, J. Preskill, P. Zoller, and B. Vermersch, Mixed-State Entanglement from Local Randomized Measurements, Phys. Rev. Lett. **125**, 200501 (2020).

[53] Y. Zhou, P. Zeng, and Z. Liu, Single-Copies Estimation of Entanglement Negativity, Phys. Rev. Lett. **125**, 200502 (2020).

[54] The only exceptions (for which the dual circuit is itself unitary) are so-called "dual-unitary" circuits [55]; these constitute a vanishing fraction of the space of all unitary evolutions.

[55] B. Bertini, P. Kos, and T. Prosen, Exact Spectral form Factor in a Minimal Model of Many-Body Quantum Chaos, Phys. Rev. Lett. **121**, 264101 (2018).

[56] B. Bertini, P. Kos, and T. Prosen, Entanglement Spreading in a Minimal Model of Maximal Many-Body Quantum Chaos, Phys. Rev. X **9**, 021033 (2019).

[57] S. Gopalakrishnan and A. Lamacraft, Unitary circuits of finite depth and infinite width from quantum channels, Phys. Rev. B **100**, 064309 (2019).

[58] B. Bertini, P. Kos, and T. Prosen, Exact Correlation Functions for Dual-Unitary Lattice Models in $1+1$ Dimensions, Phys. Rev. Lett. **123**, 210601 (2019).

[59] L. Piroli, B. Bertini, J. I. Cirac, and T. Prosen, Exact dynamics in dual-unitary quantum circuits, Phys. Rev. B **101**, 094304 (2020).

[60] P. W. Claeys and A. Lamacraft, Maximum velocity quantum circuits, Phys. Rev. Research **2**, 033032 (2020).

[61] P. Kos, B. Bertini, and T. Prosen, Correlations in Perturbed Dual-Unitary Circuits: Efficient Path-Integral Formula, Phys. Rev. X (to be published).

[62] K. Klobas, M. Vanicat, J. P. Garrahan, and T. Prosen, Matrix product state of multi-time correlations, J. Phys. A **53**, 335001 (2020).

[63] M. C. Bañuls, M. B. Hastings, F. Verstraete, and J. I. Cirac, Matrix Product States for Dynamical Simulation of Infinite Chains, Phys. Rev. Lett. **102**, 240603 (2009).

[64] M. B. Hastings and R. Mahajan, Connecting entanglement in time and space: Improving the folding algorithm, Phys. Rev. A **91**, 032306 (2015).

[65] J. Napp, R. L. La Placa, A. M. Dalzell, F. G. S. L. Brandao, and A. W. Harrow, Efficient classical simulation of random shallow 2D quantum circuits, arXiv:2001.00021.

[66] M. A. Nielsen and I. L. Chuang, *Quantum Computation and Quantum Information: 10th Anniversary Edition*, 10th ed. (Cambridge University Press, Cambridge, England, 2011).

[67] See Supplemental Material at http://link.aps.org/supplemental/10.1103/PhysRevLett.126.060501 for additional details on the spacetime duality transformation, the whole-system and subsystem purity measurement protocols, the state preparation protocol, and the quantum code properties in the mixed phase.

[68] In practice, a fully mixed state may be most easily prepared by maximally entangling the qubits in the system with a set of ancilla qubits.

[69] The iSWAP gate is defined as $e^{-i(\pi/4)(XX+YY)}$, and is equal to the product of a SWAP and a Clifford ZZ interaction $e^{i(\pi/4)ZZ}$.

[70] Because $\mathbb{E}(\ell) = 0$ and $\mathbb{E}(\ell^2)$ is finite, this random walk gives rise to diffusion. The diffusion constant diverges as p^{-2} for $p \to 0$.